ORIGINAL RESEARCH PAPER
Volume - 14 | Issue - 12 | December - 2025 | PRINT ISSN No. 2277 - 8179 | DOI : 10.36106/ijsr
INTERNATIONAL JOURNAL OF SCIENTIFIC RESEARCH

GREEN SYNTHESIS OF ZINC OXIDE NANOPARTICLES USING *THESPESIA POPULNEA* LEAF EXTRACT AND THEIR ASSOCIATION WITH ANTIBIOTICS ACTING ON METHICILLIN-RESISTANT *STAPHYLOCOCCUS AUREUS*

Medical Microbiology

Ashwini B.S. Assistant Professor, Department of Microbiology, Shri Atal Bihari Vajpayee Medical College & Research Institute, Bengaluru, Karnataka, India.

Annie M Tony Postgraduate, Department of Microbiology, Shri Atal Bihari Vajpayee Medical College & Research Institute, Bengaluru, Karnataka, India.

Bhavana V. Research Scholar, Department of Microbiology, Biotechnology and Food Technology, Jnana Bharathi Campus, Bangalore University, Bengaluru, Karnataka, India.

Lakshmeesha T.R.* Assistant Professor, Department of Microbiology, Biotechnology and Food Technology, Jnana Bharathi Campus, Bangalore University, Bengaluru, Karnataka, India. *Corresponidng Author

ABSTRACT

Background: Methicillin-resistant *Staphylococcus aureus* (MRSA) persists as a serious threat in medical science due to its multidrug resistance properties. The plant mediated zinc oxide nanoparticles (ZnO NPs) have recently been recognized as promising antibacterial agents due to their distinctive physicochemical characteristics. **Objective:** To synthesize and characterize the ZnO NPs synthesized from the *Thespesia populnea* leaf aqueous extract and to determine their activity against clinical MRSA isolates alongside antibiogram profiling. **Methods:** The fresh *T. populnea* leaves aqueous extract was used to synthesize the ZnO NPs through a solution combustion method. The ZnO NPs were further characterized using Ultraviolet-Visible Spectroscopy (UV-Vis), Fourier Transform Infrared Spectroscopy (FTIR), X-ray Diffraction (XRD), Scanning Electron Microscopy–Energy Dispersive X-ray Analysis (SEM-EDX), High-Resolution Transmission Electron Microscopy (HR-TEM), and Selected Area Electron Diffraction (SAED) analysis. A total of 62 clinical isolates were processed and identified as MRSA, along with antibiogram profiling using the VITEK 2 Compact system. Finally antibacterial activity of green-synthesized ZnO NPs against MRSA was evaluated using the Kirby–Bauer disc diffusion method. **Results:** The synthesized ZnO NPs showed their well-defined crystalline structure, hexagonal wurtzite with a nanoscale character. Among the 62 isolates, 43.5% were confirmed as MRSA, with higher rates in blood samples and high resistance to several standard antibiotics. However, the ZnO NPs showed the absence of the zone of inhibition against MRSA at the tested concentrations. **Conclusion:** The *T. populnea* mediated ZnO NPs were successfully synthesized and confirmed their ideal characteristics, but showed a lack of antibacterial properties against MRSA. These results may be due to ZnO NPs aggregation, surface chemistry, or concentration; hence, further optimization is required to improve their stability.

KEYWORDS

Methicillin-Resistant *Staphylococcus aureus*, *Thespesia populnea*, Zinc oxide nanoparticles, VITEK 2, Antibacterial activity.

INTRODUCTION

Staphylococcus aureus is a facultative anaerobic, Gram-positive bacterium that causes a broad spectrum of infections in humans. It asymptomatically colonizes the nasal and skin parts of approximately 30% of the population; however, in the healthcare environment, it is one of the five most common causes of infection that result in a serious condition [1]. In particular, nosocomial infections are mainly associated with medical devices. Over the last few years, the emergence and widespread distribution of microbial resistance to antibiotics has become a worldwide challenge in medical science. The rampant increase in antibiotic resistance among *Staphylococcus aureus* has created a global barrier to the treatment of Staphylococcal infections. Globally, Methicillin-Resistant *Staphylococcus aureus* (MRSA) bacteraemia is one of the commonest bloodstream infections, accounting for about 60–89% of nosocomial contagions with clinical complications and high mortality [2].

The intensifying occurrence of antimicrobial resistance is illustrated by MRSA, which poses a serious threat to the healthcare infrastructure due to its multiple antibiotic resistance. The MRSA are resistant to most of the β-lactam antibiotics (penicillin, cephalosporins) and also to erythromycin, clindamycin, gentamycin, ciprofloxacin, and fusidic acid to further restrict treatment therapy possibilities. Its propensity to develop biofilms makes it exceptionally resistant to most of the standard prescribed antibiotics, hence the treatment becomes more complicated [3]. According to a survey conducted by the WHO in 2024, this strain is listed on the Bacterial Priority Pathogens List, highlighting the need for novel therapeutics with multi-resistance to strengthen and control the infection. Due to the emergence of various new MRSA strains in recent decades, their resistance capacity has also evolved continuously worldwide. This evolution is responsible for the horizontal gene transfer involving mobile genetic elements such as staphylococcal cassette chromosome mec (SCCmec), which carries the mecA gene [4]. Therefore, the resistance associated with MRSA strains makes treatment problematic, and it is necessary to identify and understand the key factors influencing the development of novel medical approaches.

In modern times, metal oxide nanoparticles (NPs) are revolutionizing healthcare by introducing novel tools for antimicrobial resistance. Among them, zinc oxide (ZnO) NPs have shown promise as a therapeutic against various microbes. However, the chemical process is associated with the toxic residues that can negatively impact biomedical applications. To address these limitations, the majority of studies have focused on the green synthesis of NPs as an alternative to traditional chemical and physical methods. Since the plant contains bioactive compounds that act as capping and stabilizing agents for the synthesis of NPs, it is effective for the green synthesis of ZnO NPs [5]. Therefore, in this study, we used the *Thespesia populnea* plant as a biological source for the ZnO NPs. *T. populnea*, also known as the Indian tulip tree, a perennial tree belonging to the family Malvaceae, is widely found in coastal areas and provides medicinal value. It possesses hepatoprotective, anti-inflammatory, antioxidant, healing, immunomodulatory, memory boosting, and diuretic properties due to the presence of phytochemicals such as flavonoids, tannins, saponins, and phenols [6]. With this purpose, the objective of this study was to synthesize the ZnO NPs using *T. populnea* leaf aqueous extract and evaluate their biological effect, especially antibacterial activity against MRSA.

METHODOLOGY

Sample collection

The routine clinical samples sent to the Department of Microbiology, Shri Atal Bihari Vajpayee Medical College and Research Institute, Bangalore, for culture and antibiotic susceptibility testing according to established microbiological standards.

Isolation and characterization of MRSA

The collected specimens were inoculated on chocolate agar/blood agar, and MacConkey agar, was incubated at 37°C for 12-14 hours. Growth is observed for Gram-positive cocci (GPC) by performing a Gram stain. The GPC in clusters is subjected to catalase and coagulase tests, then processed by Vitek 2 Compact for identification, screening of MRSA by cefoxitin, and antimicrobial susceptibility testing. The confirmed MRSA isolates and their antibiograms were recorded.

Evaluation of ZnO NPs against MRSA using the disc diffusion method

These MRSA isolates were now processed on Muller-Hinton Agar (MHA) (labelled as plate 1) by lawn culture and tested for antibiotic drug discs as recommended by CLSI, such as cefoxitin, gentamicin, linezolid, ampicillin, erythromycin, clindamycin, cotrimaxazole, and ciprofloxacin by Kirby bauer disc diffusion method as ZnO NPs were tested by the disc diffusion method to maintain uniformity.

Additionally, 4 more MHA agar plates were taken and labelled as plate 2,3,4,5, respectively. All these plates were streaked by similar isolates, and similar drug discs were placed on plate 1, but plate 2 acted as a negative control, as distilled water 20 µL was placed on each drug disc to compare the activity of ZnO NPs on plates 3,4,5. ZnO NPs were reconstituted using distilled water into 3 concentrations, such as 1 mg/mL, 0.5 mg/mL, and 0.25 mg/mL, and 20 µL of each reconstitution was placed on plates 3, 4, and 5, respectively. Empty discs were placed without any antibiotic on each plate as a control. All 5 plates were incubated at 37°C overnight, and the next morning, zone sizes were measured and noted [7].

Collection and preparation of *T. populnea* leaf aqueous extract

The fresh disease-free leaves of *Thespesia populnea* were collected at Biopark, Jnana Bharathi Campus, Bangalore University, Bengaluru-560056, India. The plant authentication was carried out by experts at the Department of Botany, Jnana Bharathi Campus, Bangalore University, Bengaluru-560056, India. The selected leaves were rinsed with water 2-3 times to ensure the complete removal of dirt and then dried in a shady place until the surface moisture had evaporated. This is followed by blending the leaves with double-distilled water in a 1:3 ratio (weight to volume) using an electric blender. Then, the resulting blend was filtered using the Whatman No. 1 filter paper, and the supernatant was collected for further analysis [8].

Green synthesis of ZnO NPs using T. populnea leaf aqueous extract

The 10 g zinc nitrate hexahydrate ($Zn(NO_3)_26H_2O$) was dissolved in the 30 mL of *T. populnea* leaf aqueous extract prepared in the previous step. Transfer this solution into a crucible and place it on a heating mantle until it turns into a thick paste. The obtained paste was carefully calcinated in a preheated muffle furnace at 450°C to obtain a powder [9].

Characterization of ZnO NPs

The prepared powder was characterized by using different analytical methodologies. Initially, Ultraviolet-Visible Spectroscopy (UV-Vis) (Lab India UV-VIS 3092) analysis was performed, and the spectra were recorded from 200 to 800 nm, indicating the complete formation of the compounds. The functional groups of the compound were investigated using Fourier Transform Infrared Spectroscopy (FTIR) spectroscopy (Agilent Technologies) in the range of 4000–400 cm^{-1} through their different vibrational modes. The material identification and crystallinity were studied by powder X-ray diffraction (XRD) (Bruker D8 Advance). The Scanning Electron Microscopy–Energy Dispersive X-ray Analysis (SEM-EDX) (TESCAN-VEGA3) was performed to examine the surface morphology and elemental composition, respectively. Finally, the particle size and shape were determined using High-Resolution Transmission Electron Microscopy (HR-TEM) (Philips CM200), while the atomic arrangement was studied by Selected Area Electron Diffraction (SAED) patterns [10].

RESULTS

I. Characterization of ZnO NPs synthesized from *T. populnea* leaf aqueous extract

1. UV–Vis spectroscopy of the synthesized ZnO NPs

The spectrum from UV-Vis spectroscopy for ZnO NPs synthesized from *T. populnea* leaf aqueous extract was observed at 367 nm, as shown in Figure 1A.

2. FTIR spectrum of the synthesized ZnO NPs

Figure 1B represents the FTIR spectrum of the synthesized ZnO NPs from *T. populnea* leaf aqueous extract observed in the range 400–4000 cm^{-1}. The band at 2352 cm^{-1} is due to the stretching of the C≡C/O=C=O, while the 1972 cm^{-1} peak corresponds to the C=C=C stretching, and the band at 1383 cm^{-1} corresponds to the C–H stretching. These peaks indicate that the organic compounds present in the plant extract remained during the synthesis. Furthermore, the two other peaks at 555 cm^{-1} and 445 cm^{-1} are highly attributed to the metal oxide, i.e., ZnO stretching, confirming the formation of the ZnO Nps.

3. Powder X-Ray diffraction of the synthesized ZnO NPs

The structural and crystal nature of the NPs was effectively analysed using XRD. The well-defined diffraction pattern of the synthesized ZnO NPs is illustrated in Figure 1C. These peaks were observed at 2θ values of 31.95°, 34.62°, 36.42°, 47.71°, 56.77°,63.05°, 66.60°, 68.16°, and 69.23°, which were indexed to the (100), (002), (101), (102), (110), (103), (200), (112), and (201) crystallographic planes, respectively. These data were closely aligned with standard reference data from JCPDS card 36-1451, confirming that the synthesized ZnO NPs crystallize in a hexagonal wurtzite structure. Furthermore, the sharp and intense nature of the peaks indicates a high degree of crystallinity in the prepared samples. The average crystallite size of the ZnO NPs was estimated using the Debye–Scherrer equation, which was determined to be 10.29 ± 3.38 nm, providing a precise nanoscale estimation and confirming the nanostructured nature of the synthesized ZnO NPs.

4. SEM with EDX of the synthesized ZnO NPs

The surface morphology of the green synthesized ZnO NPs was analysed using SEM, as depicted in Figure 1D. The SEM images reveal that the nanoparticles exhibit predominantly spherical to irregular shapes with aggregation patterns. The elemental analysis, conducted through EDX, as shown in Figure 1D, confirms the presence of zinc and oxygen as the main constituents of the ZnO NPs without any impurities, as indicated by the prominent peaks in the spectrum.

5. HR-TEM with SAED of the synthesized ZnO NPs

The morphological features of the synthesized ZnO NPs were examined using HRTEM. The microscopic image revealed that the ZnO NPs were predominantly spherical to hexagonal in shape and were well-dispersed with minimal signs of agglomeration, as shown in Figure 1E. Additionally, SAED patterns Figure 1F displayed bright spotted well-defined concentric rings, which correspond to the characteristic lattice planes of wurtzite (hexagonal) ZnO, thereby confirming the crystalline nature of the NPs synthesized using synthesized from *T. populnea* leaf aqueous extract.

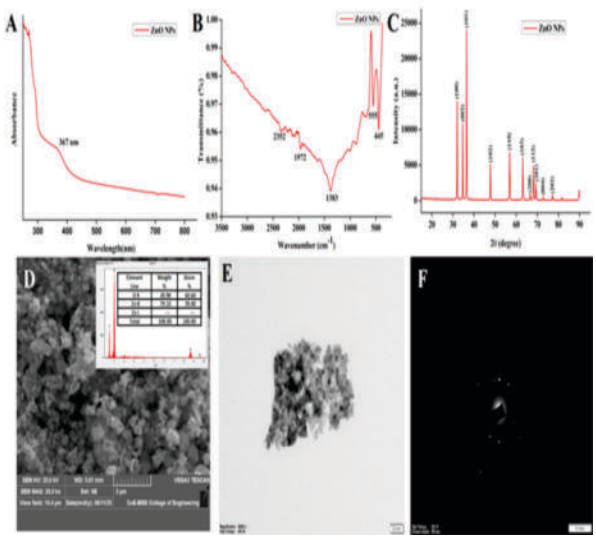

Fig 1: A) UV-Vis spectra of synthesized ZnO NPs, B) FT-IR spectrum of synthesized ZnO NPs, c) XRD pattern of synthesized ZnO NPs, D) SEM images with EDX pattern of synthesized ZnO NPs, E) HR-TEM micrographs of biosynthesized ZnO NPs, and F) SAED pattern of ZnO-NPs.

II. Sample collection

In this study, we isolated 62 samples from different clinical specimen types obtained from patients, as shown in Table 1. among the 62 isolates, MRSA was identified in 27 (43.5%) isolates, while 56.5% were non-MRSA. Interestingly, the blood samples exhibit the highest MRSA prevalence (85.7%), followed by ear discharge, sputum, and tissue (100% each; n = 1). Additionally, urine (66.7%) and ascitic fluid (33.3%) showed moderate rates of MRSA. In contrast, pus showed that the majority of the total isolates revealed a lower prevalence of about 32.6%.

Table 1: Distribution of MRSA and non-MRSA isolates among different clinical samples

Sl. No.	Specimen Type	MRSA	Non-MRSA	Total isolates	MRSA (%)	Non-MRSA (%)
1	Ascitic Fluid	1	2	3	33.3	66.7
2	Blood	6	1	7	85.7	14.3
3	Ear Discharge	0	1	1	0.0	100.0
4	Pus	14	32	46	32.6	67.4
5	Sputum	1	0	1	100.0	0.0
6	Tissue	1	0	1	100.0	0.0
7	Urine	2	1	3	66.7	33.3
	Total	25	37	62	43.5	56.5

III. Antimicrobial susceptibility profile

The resistance profile of *S. aureus* against multiple standard antibiotics is depicted in Fig 2. The results show that all the isolates exhibit 100% resistance to the HLG-Gentamicin High Level (synergy), while 96.8% resistance to P-Benzylpenicillin indicates a high level of resistance. Conversely, lower resistance rates were recorded at approximately 22.6% for each Tigecycline and Inducible Clindamycin, indicating their sensitivity to these antibiotics. Approximately 70% of the isolates were resistant to Ciprofloxacin and Erythromycin, and 60% showed resistance to Oxacillin, confirming the resistance towards the tested isolates.

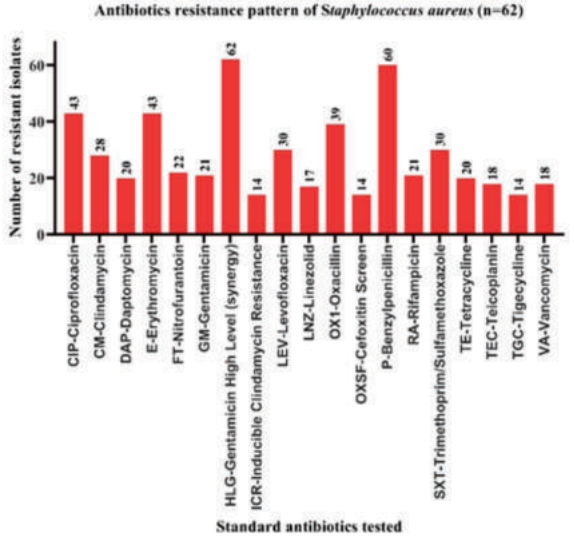

Fig 2: Resistance pattern of *S. aureus* isolates to standard antibiotics.

Antibacterial evaluation of ZnO NPs on MRSA isolates

The antibacterial activity of green-synthesized ZnO NPs against MRSA shows no zone of inhibition around the disc, whereas the standard drugs exhibit a clear zone of inhibition. This indicates the ZnO NPs have no direct antibacterial activity toward MRSA.

DISCUSSION

The UV absorption spectrum for ZnO NPs at 367 nm directly corresponds to the intrinsic band gap transition of ZnO, confirming the formation of the metal oxide. Based on a study by Gowsalya *et al*. (2017), the UV-Vis absorbance peaks for the ZnO NPs fabricated by using *T. populnea* leaf extract were observed at 295 nm. These findings support our results, but slight variations may be due to differences in particle size, synthesis process, or specific phytochemicals present in the plant extract. The peak for FTIR spectrum at 2352 cm^{-1}, 1972 cm^{-1}, and 1383 cm^{-1} indicates the presence of organic compounds, and peaks at 555 cm^{-1} and 445 cm^{-1} confirm the formation of the ZnO NPs. Similarly, a study by Sekar *et al*. (2025) reported that the FTIR spectrum of the green-synthesized ZnO NPs showed 562 cm^{-1} and 745 cm^{-1}, which correspond to vibrations of Zn-O bonds and also C-H bending vibrations 1368 cm^{-1}, these provide additional evidence of the plant role during NPs synthesis. These results collectively revealed that the prepared *T. populnea* leaf aqueous extract contains a rich source of phytochemicals, which are involved in the synthesis of NPs by donating electrons. The XRD diffraction pattern of the synthesized ZnO NPs confirmed the formation of a hexagonal wurtzite crystalline structure with an average particle size of 10.29 ± 3.38 nm. Our findings are in agreement with Moeinzadeh *et al*. (2024), who observed the XRD pattern of ZnO NPs synthesized using *Hypericum perforatum* with a particle size of 11.76 nm, further validating the structural integrity and crystallinity of biosynthesized ZnO NPs.

The SEM images revealed that the ZnO NPs were aggregated in spherical to irregular shapes, while EDX showed the presence of zinc and oxygen with no impurities. This result is consistent with the outcomes reported by Jayasri *et al*. (2025), who observed that the ZnO NPs synthesised from *T. populnea* are uniformly distributed in spherical shape using SEM analysis. The HRTEM image demonstrates that the ZnO NPs were spherical to hexagonal in shape. These results align with the studies by Umavathi *et al*. (2021), which showed HRTEM images of ZnO NPs synthesized from the aqueous extraction of *Parthenium hysterophorus*, with spherical shape, and also supporting the phase purity of the synthesized material. The absence of a zone of inhibition by ZnO NPs against certain bacterial isolates, as also observed by Souza *et al*. (2019) and Rathore *et al*. (2024) in their studies, is consistent with our findings. The antibacterial potential of the ZnO NPs is influenced by their size, shape, crystallinity, surface charges, and synthesis method [18]. Additionally, inadequate concentration, aggregation, and stability of ZnO NPs synthesized from *T. populnea* extract may account for reduced antibacterial activity. Hence, further studies are required to investigate the synthesis and physicochemical properties of the ZnO NPs.

CONCLUSION

In this study, ZnO NPs were successfully synthesized by using the *T. populnea* aqueous leaf extract. The physicochemical characterization confirms that the synthesized ZnO NPs exhibited a crystalline hexagonal wurtzite structure through UV-Vis, FTIR, XRD, SEM-EDX, HR-TEM, and SAED analyses. Among the clinical samples, 43.5% of isolates were identified as MRSA with showing significant resistance to benzylpenicillin and high-level gentamicin through the VITEK 2. However, despite their well-defined morphology and crystalline nature, the green synthesized ZnO NPs displayed no detectable antibacterial activity against MRSA, suggesting their insufficient interaction with MRSA. Therefore, further studies may focus on adjusting the ZnO NPs synthesis parameters and alternative concentrations to achieve good performance against the MRSA strains.

REFERENCES

1. Centers for Disease Control and Prevention. (2024, April 15). *Staphylococcus aureus* Basics.
2. Mishra, A., Aggarwal, A., & Khan, F. (2024). Medical device-associated infections caused by biofilm-forming microbial pathogens and controlling strategies. *Antibiotics*, *13*(7), 623.
3. Michalik, M., Podbielska-Kubera, A., & Dmowska-Koroblewska, A. (2025). Antibiotic resistance of *Staphylococcus aureus* strains-searching for new antimicrobial agents. *Pharmaceuticals*, *18*(1), 81.
4. MacFadyen, A. C., & Paterson, G. K. (2024). Methicillin resistance in *Staphylococcus pseudintermedius* encoded within novel staphylococcal cassette chromosome mec (SCC mec) variants. *Journal of Antimicrobial Chemotherapy*, *79*(6), 1303-1308.
5. Hao, Y., Wang, Y., Zhang, L., Liu, F., Jin, Y., Long, J., ... & Yang, H. (2024). Advances in antibacterial activity of zinc oxide nanoparticles against *Staphylococcus aureus*. *Biomedical Reports*, *21*(5), 161.
6. Jayasri, A., Eswara Prasad, P., Kala Kumar, B. D. P., Padmaja, K., Shivakumar, P., Anil Kumar, B., & Vidya, B. (2025). Green synthesis of silver and zinc oxide nanoparticles with *Thespesia populnea* extract and investigation of their antioxidant potential against mouse mastitis model. *Frontiers in Veterinary Science*, *12*, 1521143.
7. Khairy, T., Amin, D. H., Salama, H. M., Elkholy, I. M. A., Elnakib, M., Gebreel, H. M., & Sayed, H. A. E. (2024). Antibacterial activity of green synthesized copper oxide nanoparticles against multidrug-resistant bacteria. *Scientific Reports*, *14*(1), 25020.
8. Bhati, P., Tiwari, R., Kothari, S. L., Ray, K., Lamba, N. P., Kumar, Y., ... & Chauhan, M. S. (2025). Green synthesis of silver NPs using aqueous extract of *Artemisia scoparia* for hydrogenation of aromatic nitro compounds and their biological activity. *Frontiers in Microbiology*, *16*, 1584066.
9. Lakshmeesha, T. R., Sateesh, M. K., Prasad, B. D., Sharma, S. C., Kavyashree, D., Chandrasekhar, M., & Nagabhushana, H. (2014). Reactivity of crystalline ZnO superstructures against fungi and bacterial pathogens: Synthesized using *Nerium oleander* leaf extract. *Crystal growth & design*, 14(8), 4068-4079.
10. Jayachandran, A., Aswathy, T. R., & Nair, A. S. (2021). Green synthesis and characterization of zinc oxide nanoparticles using *Cayratia pedata* leaf extract. *Biochemistry and Biophysics Reports*, 26, 100995.
11. Gowsalya, V., Santhiya, E., & Chandramohan, K. (2017). Synthesis, characterization of ZnO nanoparticles from *Thespesia populnea*. *Indian J. Appl. Res*, *7*(10), 542-543.
12. Sekar, A., JothiMurugan, P., Shanmugam, G., Gassoumi, B., Al-Ansari, M. M., Srinivasan, P., ... & Ayachi, S. (2025). Green Synthesis and Characterization of ZnO Nanoparticles Using *Crinum asiaticum* Leaf Extracts for Biomedical Applications. *Luminescence*, *40*(4), e70158.
13. Moeinzadeh, R., Hekmati, M., Azizi, N., Qomi, M., & Esmaeili, D. (2024). Investigation of the antibacterial activity of phytosynthesized ZnO nanoparticles using *H. perforatum* extract. *Chemical Review and Letters*, *7*(2), 185-200.
14. Umavathi, S., Mahboob, S., Govindarajan, M., Al-Ghanim, K. A., Ahmed, Z., Virik, P., ... & Kavitha, C. (2021). Green synthesis of ZnO nanoparticles for antimicrobial and vegetative growth applications: A novel approach for advancing efficient high quality health care to human wellbeing. *Saudi Journal of Biological Sciences*, *28*(3), 1808-1815.
15. Souza, R. C. D., Haberbeck, L. U., Riella, H. G., Ribeiro, D. H., & Carciofi, B. A. (2019). Antibacterial activity of zinc oxide nanoparticles synthesized by solochemical process.

Brazilian Journal of Chemical Engineering, *36*(2), 885-893.
16. Rathore, M. S., Verma, H., Akhani, S. B., Pathak, J., Joshi, U., Joshi, A., ... & Oza, A. (2024). Photoluminescence and antibacterial performance of sol–gel synthesized ZnO nanoparticles. *Materials Advances*, *5*(8), 3472-3481.
17. Gudkov, S. V., Burmistrov, D. E., Serov, D. A., Rebezov, M. B., Semenova, A. A., & Lisitsyn, A. B. (2021). A mini review of antibacterial properties of ZnO nanoparticles. *Frontiers in Physics*, *9*, 641481.